$B_s \to D_s^{(*)}$ form factors from lattice QCD with $N_f = 2$ Wilson-clover quarks

Benoît Blossier[a], Pierre-Henri Cahué[b], Jochen Heitger[c], Simone La Cesa[a], Jan Neuendorf[a,c], Savvas Zafeiropoulos[d]

[a] Laboratoire de Physique des 2 Infinis Irène Joliot-Curie, CNRS/IN2P3, Université Paris-Saclay, Bâtiment 210, F-91405 Orsay Cedex, France [b] Laboratoire de Physique Subatomique et de Cosmologie, CNRS/IN2P3, 4 Allée des Martyrs, F-38000 Grenoble, France [c] Institut für Theoretische Physik, Universität Münster, Wilhelm-Klemm-Str. 9, 48149 Münster, Germany [d] Aix Marseille Univ, Université de Toulon, CNRS, CPT, Marseille, France

Abstract

We report on a two-flavor lattice QCD determination of the $B_s \to D_s$ and $B_s \to D_s^*$ transitions, which in the heavy quark limit can be parameterized by the form factors G, and h_{A_1}, h_{A_2} and h_{A_3}. In the search of New Physics through tests of lepton-flavour universality, Bs decay channels are complementary to B decays and widely studied at B factories and LHCb. The purpose of our study is to explore a suitable method to extract form factors associated with $b \to c$ currents from lattice QCD. In particular, we present numerical results for G and h_{A_1}.

Introduction

We consider the semi leptonic decay B_s to $D_s^{(*)}$ with both mesons at rest.

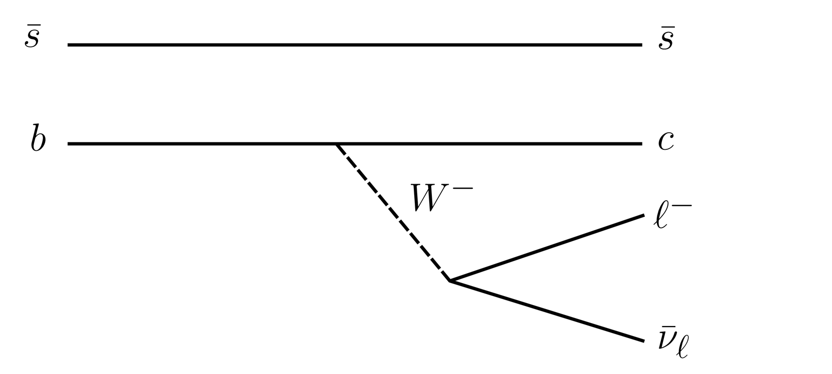

Figure 1: Schematic of the decay $\bar{B}_s^0 \to D_s^{+(*)} \ell^- \bar{\nu}_\ell$

The decay width includes the CKM matrix element V_{cb} as well as a QCD form factor. We focus on $B_s \to D_s$, where this factor is called G. It is h_{A_1} for $B_s \to D_s{}^*$

$$\frac{d\Gamma_{B_s \to D_s}}{dw} \propto |V_{cb}|^2 \cdot |\mathrm{G(w)}|^2 \qquad (1)$$

The decay can be parametrized as

$$\langle D_s(k)|\bar{b}\gamma_\mu c|B_s(p)\rangle = A_\mu(p,k)\,\mathrm{G(w)} + B_\mu(p,k) f_0(w), \qquad (2)$$

where $w = \frac{E_{D_s}}{m_{D_s}}$ is the relative velocity of the D_s meson.

Data

The correlators were measured on eight CLS ensembles with $N_f = 2$.

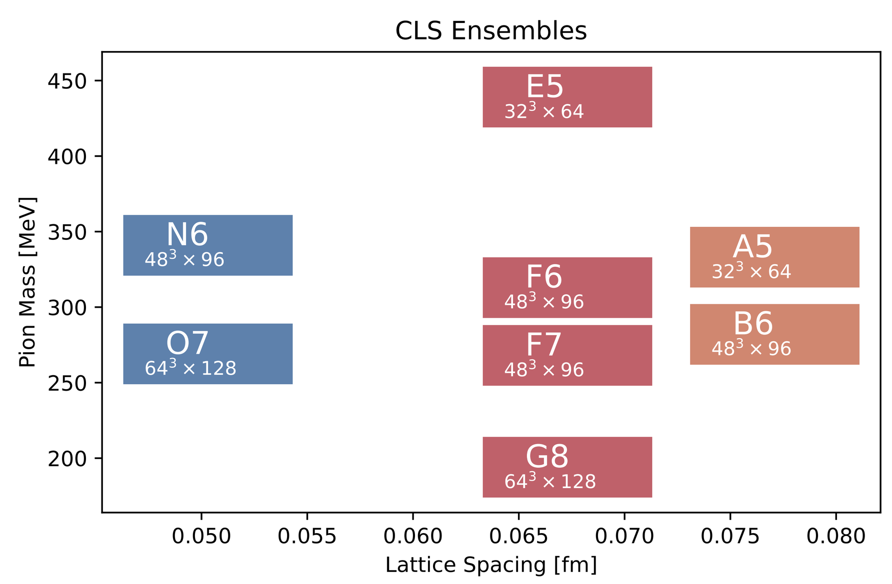

Figure 2: Parameters of the different Ensembles.

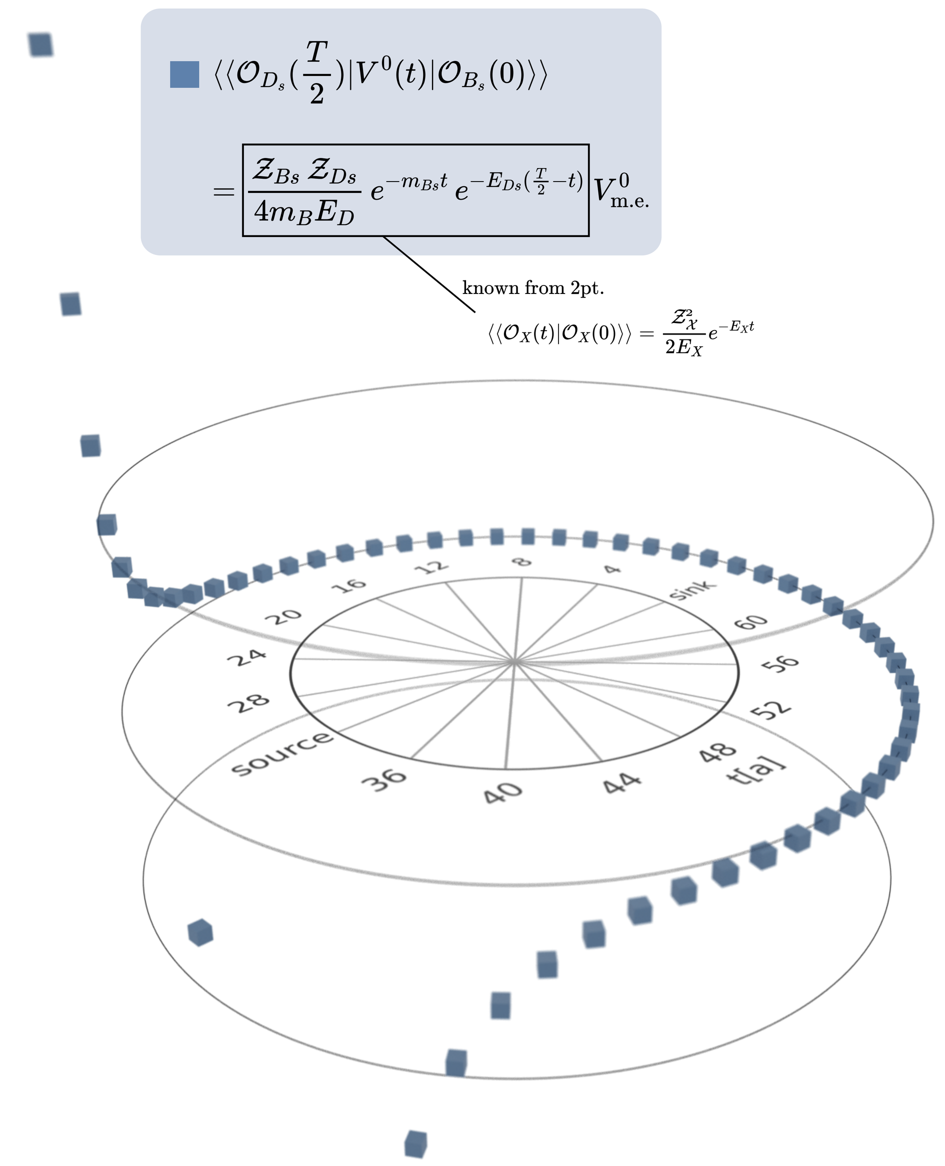

Figure 3: Examplatory three point correlator. Cylindical coordinates to emphasize periodic time axis.

To get the matrix elements corresponding to semi leptonic decays, we need three point correlators. The source and sink are kept at maximum distance $\frac{T}{2}$, while the operator inbetween is varied.

GEVP

To improve the overlap with the ground state, each observable is measured for 4×4 smearing levels. To get the eigenvectors, we solve the GEVP for the two point correlators, where the source and sink are identical.

$$v^T_{D_s^{(*)}} \langle\langle D_s^{(*)}(t)|D_s^{(*)}(0)\rangle\rangle_{i,j} v_{D_s^{(*)}} \propto e^{-E_{D_s^{(*)}}t}$$
$$v^T_{B_s} \langle\langle B_s(t)|B_s(0)\rangle\rangle_{i,j} v_{B_s} \propto e^{-m_{B_s}t} \qquad (3)$$

We can then project the three point correlator with those vectors.

$$v^T_{D_s^{(*)}} \langle\langle D_s^{(*)}|O^\mu|B_s\rangle\rangle_{i,j} v_{B_s} \qquad (4)$$

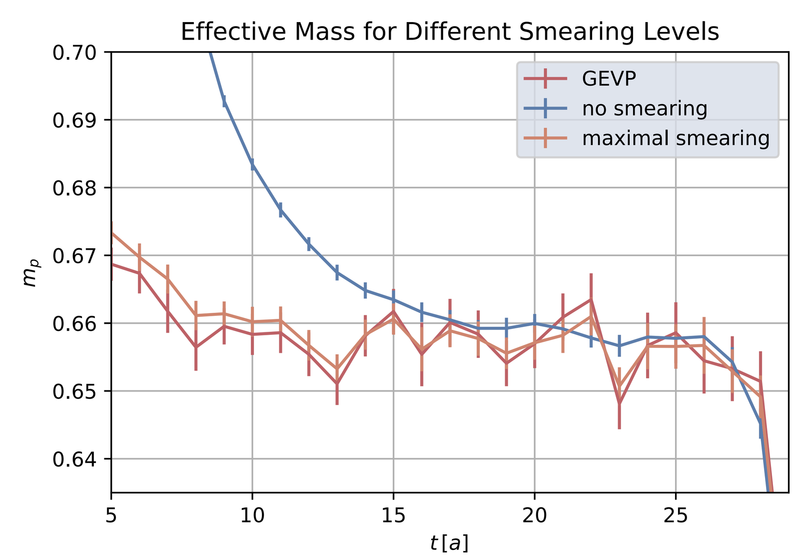

Figure 4: Demonstration of the effect of the GEVP on the plateau of the effective mass.

Extrapolation to $w = 1$

Eq.2 can not be solved for G at zero recoil. We perform the extrapolation of G at different D_s momenta and extrapolate to $w = 1$.

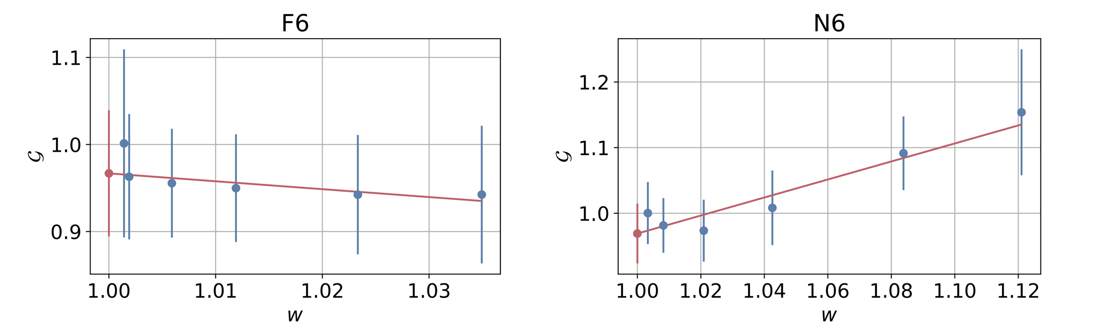

Figure 5: Linear extrapolation of G to the zero recoil point for two ensembles.

The form factor h_{A_1} can be extracted directly at $w = 1$.

Mass Step Scaling

None of the correlators were measured directly at the b-quark scale. Instead six different heavy quark masses were tuned so that the ratios between the pseudoscalar masses are constant:

$$m_{H_s(h)} = m_{D_s}\left(\frac{m_{B_s}}{m_{D_s}}\right)^{\frac{h}{6}}. \qquad (5)$$

The analysis was performed seperately for each quark mass. We then extrapolate the final result to the physical B_s mass. This approach is especially interesting for $B_s \to D_s$. In the elastic case G is one by definition.

$$G_{B_s} = \prod_{h=0}^{6} \sigma_h \quad \text{with} \quad \sigma_h = \frac{G_{h+1}}{G_h} \qquad (6)$$

Some correlations as well as renormalization factors can be avoided by only considering the ratios.

Extrapolation to the physical point

G and h_{A_1} must be extrapolated to the physical point. We use the simple ansatz

$$O = O^0 + O^1\left(\frac{a}{a_{\beta=5.3}}\right)^2 + O^2\left(\frac{m_\pi}{m_\pi^{\mathrm{phys}}}\right)^2. \qquad (7)$$

This is done for each quark mass independently.

Results

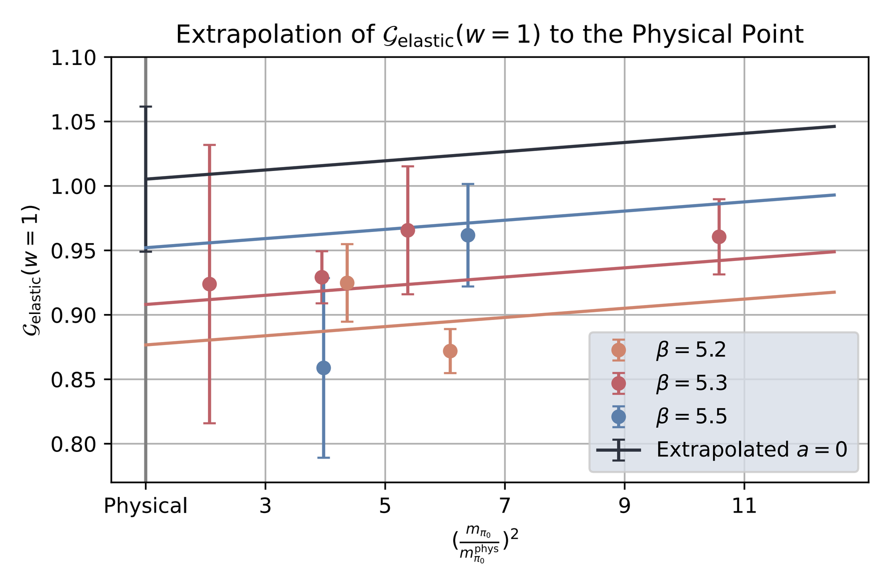

Figure 6: Check, that G_{elastic} is compatible with one at the physical point.

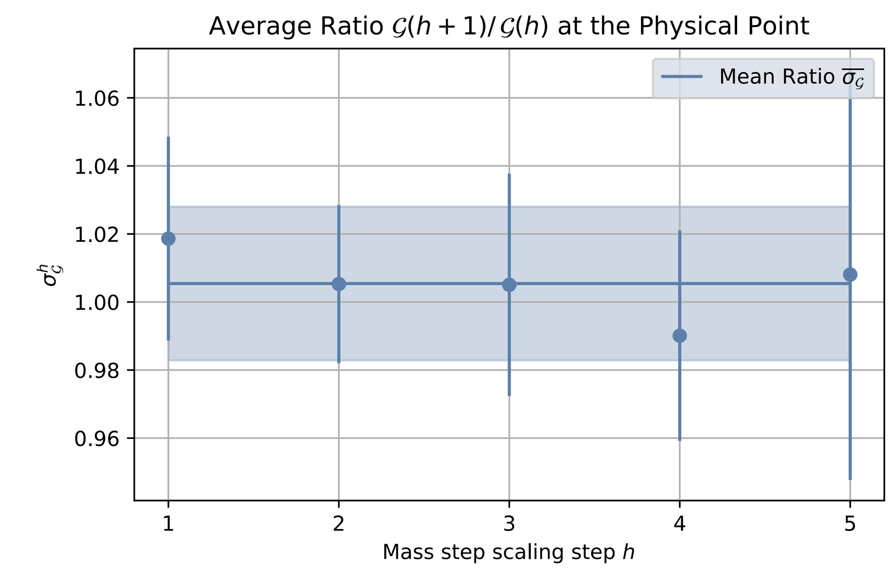

Figure 7: Ratios $\frac{G_{h+1}}{G_h}$ at different mass step scaling steps.

The ratios are compatible with a mean value.

$$G_{B_s} = \bar{\sigma}^6 = 1.03(14) \qquad (8)$$

The same is done for h_{A_1} with the difference being, that it is not equal to one if $m_{H_s(h)} = m_{D_s}$.

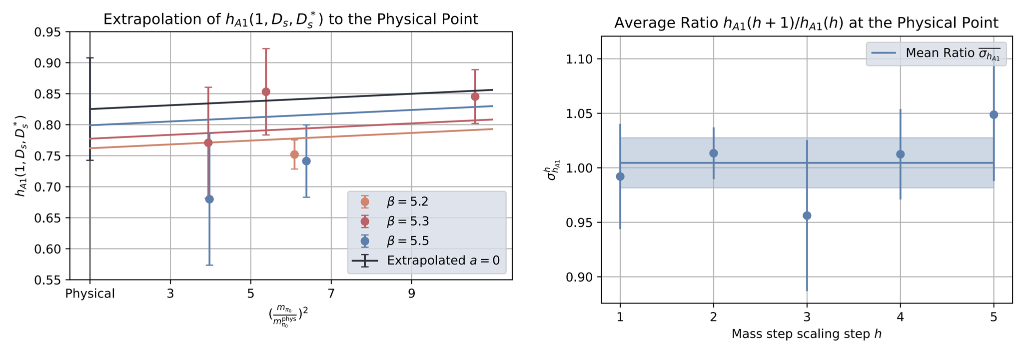

Figure 8: Analogous extrapolation of h_{A_1}

We get the result:

$$h_{A_1} = h_{A_1}^{D_s^* \to D_s} \overline{\sigma_{h_{A_1}}}^6 = 0.85(16) \qquad (9)$$

Discussion

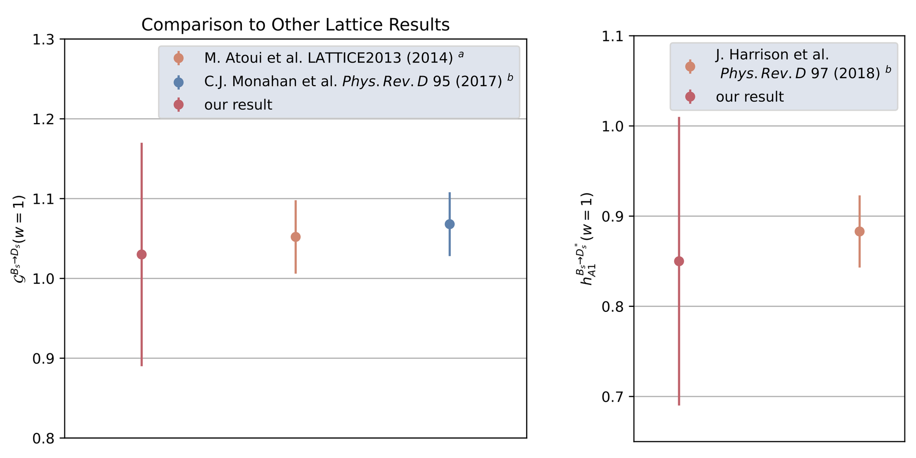

Figure 9: Comparison of G and h_{A_1} to published lattice results using [a] $N_f = 2$ twisted-mass fermions and [b] staggered fermions with non-relativistic b-quark.

We show, that we can control:

- cut-off effects using mass step scaling
- excited states using the GEVP
- $w \to 1$ using a linear extrapolation

The large statistical error was estimated independently with binning and the Γ-method. The source-sink separation of $\frac{T}{2} > 2$ fm may be reduced to improve it. The GEVP results are mostly consistent with the most smeared operators, which could be used exclusively to reduce costs.